

# Using Dicyanoanthracene Triflates as Superior Precursors: Modifying Properties by Sterically Hindered Aryl Substituents

Florian Glöcklhofer,<sup>\*[a]</sup> Paul Kautny,<sup>[a]</sup> Patrick Fritz,<sup>[a]</sup> Berthold Stöger,<sup>[b]</sup> and Johannes Fröhlich<sup>[a]</sup>

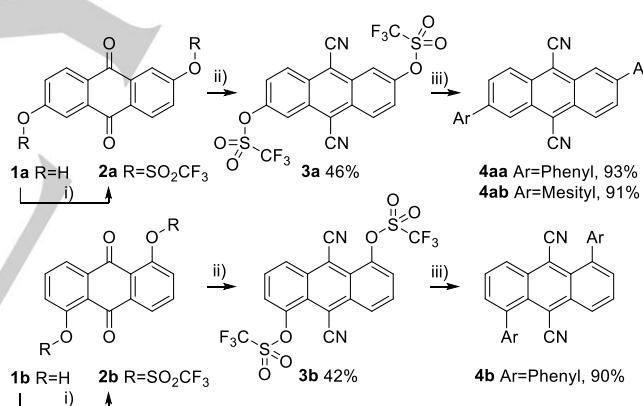
**Abstract:** The preparation of 9,10-dicyanoanthracene triflates is reported. Taking advantage of the high reactivity of these precursors in Suzuki coupling reactions, sterically hindered substituents are introduced. The impact of the substituents on the crystallographic and photophysical properties is investigated. The results highlight the usefulness of the new triflates and the substituents for the development of 9,10-dicyanoanthracene based materials.

The international community has agreed on significantly cutting the greenhouse gas emissions in an initiative to fight climate change.<sup>[1]</sup> Developing new technologies for a more responsible and efficient consumption of energy is an important part of this agreement. Organic light emitting diodes for lighting applications represent such a new technology that could improve the energy efficiency.<sup>[2]</sup> There is an ongoing quest for new emitters to further develop this technology.

Anthracene is one of the most investigated building blocks for fluorescent emitters, due to the facile synthesis and the good emission properties of many anthracene derivatives.<sup>[3]</sup> However, the particularly promising 9,10-dicyanoanthracene (DCA) has been neglected in studies of organic light emitting diodes for a reason. The planar molecular structure allows for strong intermolecular interactions and favors aggregation. This ultimately results in a broad and distinctly redshifted emission and in low efficiency in the solid state compared to the very high fluorescence quantum yield of the blue emission in solution.<sup>[4]</sup> Additional bulky, sterically hindered substituents can prevent this aggregation and the close assembly of the anthracene cores. The resulting twisted molecular configuration after introduction of such substituents can also decrease the expansion of the  $\pi$ -electron system, which otherwise drastically impacts the emission properties and again leads to a redshifted emission.<sup>[5]</sup> Until recently, there was no reasonable possibility to carry out such modifications on a DCA core. This changed when we reported on a new synthesis of cyanoarenes from the corresponding quinones.<sup>[6]</sup> For the first time, this synthesis enables a straightforward preparation of halogenated DCAs, which can be used as precursors for the introduction of aryl substituents by coupling reactions. However, the introduction of

sterically hindered substituents is often ambitious and the very poor solubility of the halogenated DCAs represents an additional challenge for a fast and efficient reaction. Consequently, the aim of this work was to develop DCA precursors with a higher reactivity in Suzuki coupling reactions.

Triflates are known to be valuable alternatives to halogenated precursors. Although they were reported to be less reactive,<sup>[7]</sup> we expected a higher solubility and thus an improved reactivity for the DCA triflates compared to the halogenated analogs. In order to verify this assumption, 2,6-triflate **3a** and 1,5-triflate **3b** were selected for preparation (Scheme 1). **3a** allows for a comparison to the previously used brominated precursor by coupling with phenylboronic acid,<sup>[6a]</sup> but also enables to investigate the introduction of sterically hindered substituents by coupling with mesitylboronic acid. Coupling **3b** and phenylboronic acid reveals the influence of steric hindrance by the spatial proximity of the cyano groups.



**Scheme 1.** i) Synthesis of anthraquinone triflates **2a** and **2b**; conditions: triflic anhydride, pyridine, overnight, 0 °C to rt.<sup>[8]</sup> ii) Preparation of dicyanoanthracene triflates **3a** and **3b**; conditions: a) TMSCN, *n*-butyllithium, 15 min, rt; b) addition to anthraquinone triflate, DMF, 3 h, rt; c) addition of MeCN, PBr<sub>3</sub>, overnight, 50 °C. iii) Suzuki coupling with boronic acids; conditions: Pd(PPh<sub>3</sub>)<sub>4</sub>, aq. K<sub>2</sub>CO<sub>3</sub>, THF, argon, 30 min (**4aa**, **4b**) / 90 min (**4ab**), reflux.

The synthesis of triflates **3a** and **3b** was carried out in two steps (Scheme 1). In the first step, anthraquinone triflates **2a** and **2b** were prepared starting from the two dihydroxy anthraquinones **1a** and **1b** (anthraflavic acid and anthrarufin). In contrast to the preparation of the halogenated analogs, this reaction can be easily carried out on a multigram scale.<sup>[6]</sup> In the second step, the cyano groups were introduced. This reaction proceeds *via* the intermediate formation of silylated cyanohydrins using trimethylsilyl cyanide (TMSCN) and subsequent aromatization.<sup>[6]</sup> Lithium cyanide was used to catalyze the formation of the silylated cyanohydrins. This catalyst was prepared *in-situ* by adding *n*-butyllithium to the TMSCN prior to the addition to the

[a] F. Glöcklhofer, P. Kautny, P. Fritz, Prof. Dr. J. Fröhlich  
Institute of Applied Synthetic Chemistry, TU Wien  
Getreidemarkt 9/163, 1060 Vienna, Austria  
E-mail: florian.gloecklhofer@tuwien.ac.at

[b] Dr. B. Stöger  
Institute of Chemical Technologies and Analytics, TU Wien  
Getreidemarkt 9/164, 1060 Vienna, Austria

Supporting information for this article is given via a link at the end of the document. CCDC-1500690-1500694 and 1517671 contain the supplementary crystallographic data for this paper. These data can be obtained free of charge from The Cambridge Crystallographic Data Centre via [www.ccdc.cam.ac.uk/data%5Frequest/cif](http://www.ccdc.cam.ac.uk/data%5Frequest/cif).

anthraquinone substrates. The *trans* configuration of the cyanohydrin intermediate of **3b** was confirmed by X-ray diffraction (see Supporting Information). The aromatization was carried out by diluting the reaction with acetonitrile and adding  $\text{PBr}_3$  as reagent. As expected, **3a** and **3b** are significantly more soluble than the halogenated DCAs, enabling purification by column chromatography.

The structures of both DCA triflates were confirmed by X-ray diffraction (Figure 1, see Supporting Information for detailed crystal descriptions). The triflate groups are not bulky enough to inhibit  $\pi$ - $\pi$ -interaction in **3a**, as shown by short C-C distances of 3.41 Å. In **3b**, the intermolecular contact is established *via* the cyanide groups.

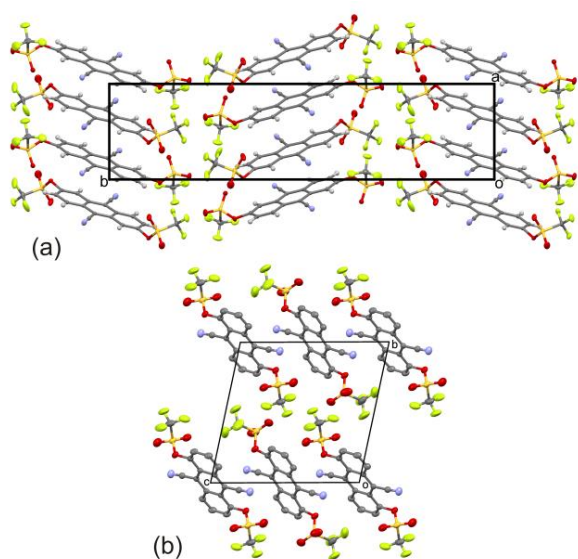


**Figure 1.** The crystal structures of **3a** (a) and **3b** (b). C (grey), N (blue), O (red), S (yellow), and F (green) atoms are represented by ellipsoids drawn at the 50% probability levels. H atoms and the disorder of the **3b** molecules were omitted for clarity.

Screening reactions confirmed the significantly enhanced reactivity of **3a** and **3b** in Suzuki coupling reactions (Table 1). Using  $\text{Pd}[(\text{PPh}_3)_4]$  as catalyst, an aqueous  $\text{K}_2\text{CO}_3$  solution as base, and THF as solvent, full conversion was observed for the formation of **4aa** in less than 90 min at room temperature. At 55 °C the same reaction was complete in less than 15 min, considerably faster than the previously observed 3 h for the brominated precursor under the same conditions.<sup>[6a]</sup>

As expected, the introduction of the sterically hindered mesityl substituents to obtain **4ab** was more ambitious; but still, this reaction was complete after stirring overnight at room temperature. At 55 °C full conversion was observed in less than 60 min. In contrast, the steric hindrance by the cyano groups did not affect the reaction rate for the synthesis of **4b**.

Considering these results, the synthesis of **4aa**, **4ab**, and **4b** on a preparative scale was carried out under reflux (Scheme 1). Yields of 90%+ were obtained for all three target compounds after purification by column chromatography.

**Table 1.** Screening reactions for the Suzuki coupling of triflates **3a** and **3b** (1.00 equiv) and boronic acids (2.50 equiv) carried out on a 0.05 mmol scale in a heating block; conditions:  $\text{Pd}[(\text{PPh}_3)_4]$  (0.05 equiv),  $\text{K}_2\text{CO}_3$  (5.00 equiv, 2.0 M in  $\text{H}_2\text{O}$ ), THF (0.05 M), argon.

| Product    | Triflate  | Boronic acid | Substituent positions | Reaction temperature | Reaction time <sup>[a]</sup> |
|------------|-----------|--------------|-----------------------|----------------------|------------------------------|
| <b>4aa</b> | <b>3a</b> | Phenyl       | 2,6                   | rt<br>55°C           | <90 min<br><15min            |
| <b>4ab</b> | <b>3a</b> | Mesityl      | 2,6                   | rt<br>55°C           | overnight<br><60 min         |
| <b>4b</b>  | <b>3b</b> | Phenyl       | 1,5                   | rt<br>55°C           | <90 min<br><15 min           |

[a] Time until full conversion of both triflate functionalities, determined by thin-layer chromatography.

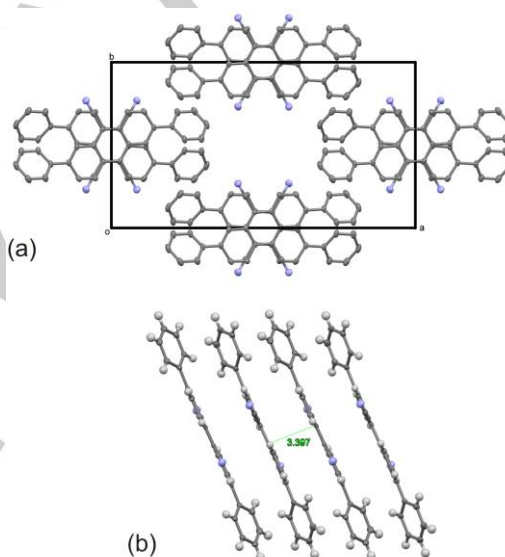


**Figure 2.** (a) The crystal structure of **4aa** (viewed down [001]). H atoms and the disordered solvent molecules were omitted for clarity. (b) Rods of **4aa** molecules connected by  $\pi$ - $\pi$  interactions extending along [001]. Color codes as in Figure 1.

Analysis of single crystals revealed that for **4aa** the molecules are connected by strong  $\pi$ - $\pi$  interactions (C7...C7: 3.397 Å) to rods extending along [001] (Figure 2). This is no surprise, due to the absence of sterically hindered substituents. **4aa** crystallizes with 0.575  $\text{CHCl}_3$  molecules in space group  $C2/c$ . One crystallographically unique **4aa** molecule is located on a center of inversion ( $Z' = \frac{1}{2}$ ). The phenyl substituents are slightly inclined with respect to the anthracene ring [angle of least-square planes:  $29.96(8)^\circ$ ]. In the free space of the packing  $\text{CHCl}_3$  solvent molecules are located, which are disordered around a twofold axis.

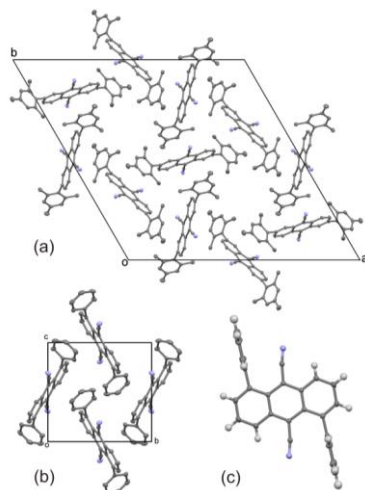


**Figure 3.** The crystal structures of **4ab** (a) (viewed down [001]) and **4b** (b) (viewed down [100]). (c) Molecular structure of **4b**. H atoms are represented by spheres of arbitrary radius. Color codes as in Figure 1.

For compounds **4ab** and **4b** the  $\pi$ -stacking is efficiently inhibited by the sterically hindered substituents (Figure 3). **4ab** crystallizes from  $\text{CDCl}_3$  in the  $R\bar{3}$  space group with one **4ab** molecule located on a center of inversion. A solvent molecule is disordered around the  $\bar{3}$  rotoinversion. **4b** crystallizes in the  $P2_1/c$  space group with one molecule located on a center of inversion. The substituents of both compounds are virtually perpendicular to the anthracene [angle of least-squares planes:  $88.38(7)^\circ$  (**4ab**) and  $89.26(4)^\circ$  (**4b**)]. The phenyl substitution next to the cyano group results in a remarkable bending of the latter

[C-C-N:  $172.11(11)^\circ$  for **4b** vs.  $179.00(16)^\circ$  for **4ab**]. The absence of  $\pi$ -stacking validates the general strategy and is in sharp contrast to both **4aa** and the plain DCA.<sup>[9]</sup>

UV/VIS absorption and photoluminescent emission spectra of the target compounds and the plain DCA were recorded to investigate the impact of the phenyl and mesityl substituents on the photophysical properties. Key parameters are summarized in Table 2. All compounds exhibit a distinct absorption maximum (between 261 nm and 306 nm) and four less intense absorption bands (between 356 nm and 447 nm) in solution (Figure 4, left). The latter are systematically redshifted for the substituted DCA derivatives. The bands of the phenyl substituted **4aa** and **4b** are located in close proximity, whereas the corresponding transitions of **4ab** are less redshifted. This is also reflected in the absorption onsets and the related optical bandgaps. **4aa** (2.67 eV) and **4b** (2.65 eV) exhibit the smallest bandgap, while the value of **4ab** (2.79 eV) is located exactly in between these values and the bandgap of the DCA (2.92 eV). These results indicate that the  $\pi$ -electron system of the DCA is expanded by the two additional phenyl substituents. However, this effect is significantly reduced in **4ab**, due to increased torsion resulting from the steric demand of the mesityl substituents.

With some exceptions, similar results were obtained for the photoluminescence in *n*-heptane solution (Figure 4, middle). The emission of **4aa** is significantly redshifted ( $\lambda_{\text{max}}=460$  nm) compared to the DCA ( $\lambda_{\text{max}}=419$  nm); the emission maximum of **4ab** ( $\lambda_{\text{max}}=447$  nm) is located in between. In contrast to the absorption, **4b** ( $\lambda_{\text{max}}=476$  nm) exhibits a more pronounced redshift than **4aa**. The photoluminescence quantum yields in solution relative to DCA (90%<sup>[4b]</sup>) are affected by the substituents, but the quantum yields are still high.

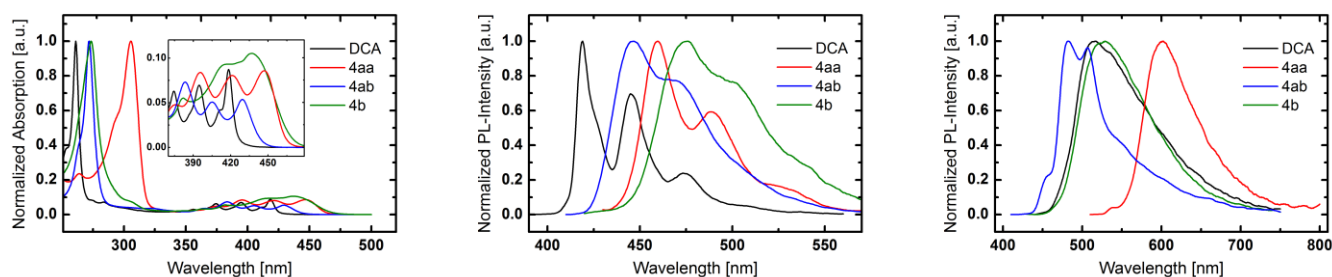


**Figure 4.** UV/VIS absorption (left) and photoluminescent emission spectra in *n*-heptane solutions (middle) and from powders (right) of **4aa**, **4ab**, **4b** and DCA.

**Table 2.** Key physical and theoretical parameters of the materials under investigation.

| Product    | $\lambda_{\text{abs,Sol}}^{\text{[a]}}$ [nm] | $\lambda_{\text{PL,Sol}}^{\text{[a]}}$ [nm] | $Q_{\text{PL,Sol}}^{\text{[a]}}$ | $\lambda_{\text{PL,Pow}}^{\text{[b]}}$ [nm] | $\Delta E_{\text{opt}}^{\text{[a]}}$ [eV] | HOMO/LUMO <sup>[c]</sup> [eV] | $\Delta E_{\text{cal}}^{\text{[c]}}$ [eV] |
|------------|--|---|----------------------------------|---|---|-------------------------------|---|
| <b>DCA</b> | <b>261</b> /356/374/395/418 <sup>[d]</sup>   | <b>419</b> /445/473 <sup>[d]</sup>          | 90% <sup>[4b]</sup>              | <b>516</b> <sup>[d]</sup>                   | 2.92                                      | -6.42/-3.32                   | 3.10                                      |
| <b>4aa</b> | <b>306</b> /376/396/421/447 <sup>[d]</sup>   | <b>460</b> /488/529 <sup>[d]</sup>          | 79% <sup>[e]</sup>               | <b>601</b> <sup>[d]</sup>                   | 2.67                                      | -6.15/-3.25                   | 2.90                                      |
| <b>4ab</b> | <b>272</b> /366/383/405/429 <sup>[d]</sup>   | <b>447</b> /469 <sup>[d]</sup>              | 81% <sup>[e]</sup>               | 456/ <b>482</b> /507 <sup>[d]</sup>         | 2.79                                      | -6.26/-3.20                   | 3.06                                      |
| <b>4b</b>  | <b>274</b> /364/382/416/437 <sup>[d]</sup>   | <b>476</b> /499 <sup>[d]</sup>              | 71% <sup>[e]</sup>               | <b>529</b> <sup>[d]</sup>                   | 2.65                                      | -6.07/-3.15                   | 2.92                                      |

[a] Determined in *n*-heptane solutions. [b] Determined from powder samples. [c] Calculated applying density functional theory level (B3LYP/6-311G(d,p)). [d] Bold indicates maximum. [e] Relative to DCA.

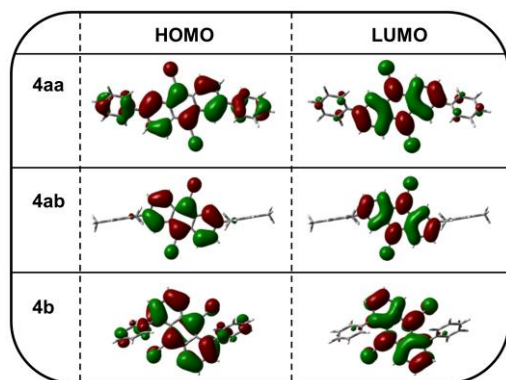


Figure 5. Spatial distribution of HOMO and LUMO levels of **4aa**, **4ab** and **4b**.

DFT calculations were employed to shed further light on the properties of the materials. The trends for the calculated HOMO/LUMO gaps and for the experimentally determined optical bandgaps in solution are in excellent agreement. For both phenyl substituted compounds, the HOMO clearly expands onto the aryl substituents (Figure 5, top and bottom), which explains the increased energy level and the smaller bandgap compared to the DCA. In contrast, the HOMO of **4ab** is exclusively located on the DCA core (Figure 5, middle) as a result of the perpendicular orientation of the sterically demanding mesityl substituents. Similar observations were made for the LUMO levels, but with a distinctly stronger localization of the orbital at the DCA core for all materials under investigation. The DFT calculations also revealed through-space interactions of the phenyl substituents and the cyano groups in **4b** (see Supporting Information), which is a possible explanation for the pronounced redshift of the emission in solution and for the expansion of the HOMO onto the substituents despite their perpendicular orientation.

The advantages of the sterically hindered substituents come to the fore when switching from the solution to the solid state. Photoluminescence spectra of powder samples (Figure 4, right) proved the tremendous effect of the packing motif on the solid state emission. The emission maximum of **4ab** (482 nm) is redshifted by only 35 nm compared to the solution. In contrast, the maximum of the  $\pi$ -stacked plain DCA (516 nm) is distinctly shifted by 97 nm, resulting in a reversed order of the emission maxima compared to the measurements in solution. The packing effects also result in a reversed order of the emission maxima of the phenyl substituted DCAs; **4b** (529 nm) exhibits a shift of 53 nm, the maximum of **4aa** (601 nm) is shifted by 141 nm. The large redshift of **4aa** is attributed to the strong  $\pi$ - $\pi$  interactions observed in the crystal structure.

In conclusion, our investigations illustrate the tremendous effect of sterically hindered aryl substituents on the properties of DCA. The acquired knowledge will guide the molecular design of DCA based materials for organic light emitting diodes and other applications. The careful selection of substituents, which take into account the packing effects, but also the charge transport properties, is considered a promising approach. The newly developed, highly reactive DCA triflates will enable a facile preparation of new DCA based materials.

## Experimental Section

Experimental and instrumental details for the synthesis and characterization of all compounds, as well as for the DFT calculations are provided in the Supporting Information.

**General procedure for the synthesis DCA triflates **3a** and **3b****  
*n*-Butyllithium (0.10 equiv, 2.5 M in hexanes) was added carefully to rigorously stirred TMSCN (2.20 equiv) in a sealed reaction vial at room temperature. After 15 min, the resulting mixture was added to anthraquinone triflate **2a** / **2b** (1.00 equiv), again at room temperature. Dry DMF (0.5 ml mmol<sup>-1</sup> starting material) was used to fully transfer the residues of the mixture. The reaction stirred at room temperature for 3 h. MeCN (3.0 ml mmol<sup>-1</sup> starting material) and PBr<sub>3</sub> (1.20 equiv) were added and the reaction was heated to 50°C overnight. The reaction was then allowed to cool to room temperature, diluted with CH<sub>2</sub>Cl<sub>2</sub> and directly filtered over a pad of silica (conditioned with CH<sub>2</sub>Cl<sub>2</sub> and some drops of MeCN) using CH<sub>2</sub>Cl<sub>2</sub> as eluent. After evaporation of the solvent, the residue was purified by column chromatography (petroleum ether:CH<sub>2</sub>Cl<sub>2</sub> 7:3 to 3:2). Yields of 46% (**3a**) / 42% (**3b**) were obtained.

**General procedure for the synthesis of **4aa**, **4ab**, and **4b****  
 DCA triflate **3a** / **3b** (1.00 equiv) and phenylboronic acid (2.50 equiv) were mixed in degassed THF (0.05 M) under argon atmosphere and heated to reflux. An aqueous K<sub>2</sub>CO<sub>3</sub> solution (5.00 equiv, 2.0 M) and Pd(PPh<sub>3</sub>)<sub>4</sub> (0.05 equiv) were added and the reaction was stirred for 30 min (**4aa**, **4b**) / 90 min (**4ab**). After cooling to room temperature, the reaction was poured on water and extracted four times with CH<sub>2</sub>Cl<sub>2</sub>. The combined organic layers were dried over sodium sulfate and the solvent was evaporated in vacuo. After evaporation of the solvent, the residue was purified by column chromatography (petroleum ether:CH<sub>2</sub>Cl<sub>2</sub> 3:2). Yields of 90%+ were obtained for all three target compounds.

## Acknowledgements

This work was supported in part by the TU Wien "Innovative Projects" research funds. The X-ray center of the TU Wien is acknowledged for providing access to the single-crystal diffractometer. We gratefully thank Manuel Spettel for contributing to synthetic experiments and Christian Hametner for NMR measurements.

**Keywords:** cross-coupling • cyanides • fluorescence • fused-ring systems • steric hindrance

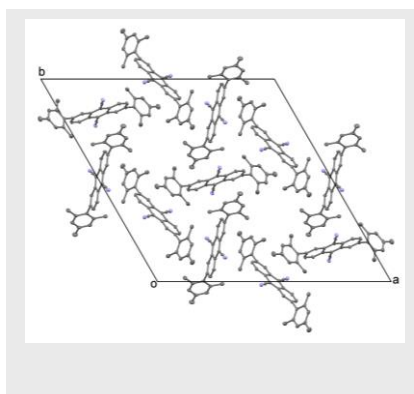
- [1] UNFCCC, *Adoption of the Paris Agreement FCCC/CP/2015/L.9/Rev.1* **2015**.
- [2] a) S. Reineke, F. Lindner, G. Schwartz, N. Seidler, K. Walzer, B. Lüsse, K. Leo, *Nature* **2009**, *459*, 234-238; b) S. Reineke, M. Thomschke, B. Lüsse, K. Leo, *Rev. Mod. Phys.* **2013**, *85*, 1245-1293; c) N. Thejokalyani, S. J. Dhole, *Renewable and Sustainable Energy Rev.* **2014**, *32*, 448-467.
- [3] a) J. Huang, J.-H. Su, H. Tian, *J. Mater. Chem.* **2012**, *22*, 10977-10989; b) M. Zhu, C. Yang, *Chem. Soc. Rev.* **2013**, *42*, 4963-4976.
- [4] a) S. Ateşli, A. Yildiz, *J. Chem. Soc., Faraday Trans. 1* **1983**, *79*, 2853-2861; b) S. Schoof, H. Güsten, C. Von Sonntag, *Berichte der Bunsengesellschaft für physikalische Chemie* **1978**, *82*, 1068-1073.
- [5] a) K. H. So, H.-T. Park, S. C. Shin, S.-G. Lee, D. H. Lee, K.-H. Lee, H.-Y. Oh, S.-K. Kwon, Y.-H. Kim, *Bull. Korean Chem. Soc.* **2009**, *30*, 1611-1615; b) K.-R. Wee, W.-S. Han, J.-E. Kim, A.-L. Kim, S. Kwon, S. O. Kang, *J. Mater. Chem.* **2011**, *21*, 1115-1123; c) M. A. Reddy, A. Thomas, K. Srinivas, V. J. Rao, K. Bhanuprakash, B. Sridhar, A. Kumar,

- M. N. Kamalasanan, R. Srivastava, *J. Mater. Chem.* **2009**, *19*, 6172-6184; d) C.-L. Wu, C.-H. Chang, Y.-T. Chang, C.-T. Chen, C.-T. Chen, C.-J. Su, *J. Mater. Chem. C* **2014**, *2*, 7188-7200.
- [6] a) F. Glöckhofer, M. Lunzer, B. Stöger, J. Fröhlich, *Chem. – Eur. J.* **2016**, *22*, 5173-5180; b) F. Glöckhofer, M. Lunzer, J. Fröhlich, *Synlett* **2015**, *26*, 950-952.
- [7] T. Ohe, N. Miyaura, A. Suzuki, *J. Org. Chem.* **1993**, *58*, 2201-2208.
- [8] J. E. Gautrot, P. Hodge, D. Cupertino, M. Helliwell, *New J. Chem.* **2007**, *31*, 1585-1593.
- [9] J. Xiao, Z. Yin, B. Yang, Y. Liu, L. Ji, J. Guo, L. Huang, X. Liu, Q. Yan, H. Zhang, Q. Zhang, *Nanoscale* **2011**, *3*, 4720-4723.

WILEY-VCH

## COMMUNICATION

**Get rid of the  $\pi$ -stack!** Highly reactive dicyanoanthracene triflates enable a fast introduction of sterically hindered aryl substituents by Suzuki coupling reactions. The substituents drastically impact the packing motif and the emission characteristics of dicyanoanthracene.



Florian Glöcklhofer,\* Paul Kautny,  
Patrick Fritz, Berthold Stöger, and  
Johannes Fröhlich

Page No. – Page No.

**Using Dicyanoanthracene Triflates as  
Superior Precursors: Modifying  
Properties by Sterically Hindered Aryl  
Substituents**

WILEY-VCH